Cell Metabolism, Volume *31*

Supplemental Information

Deamidation Shunts RelA from Mediating Inflammation to Aerobic Glycolysis

Jun Zhao, Mao Tian, Shu Zhang, Alireza Delfarah, Ruoyun Gao, Youliang Rao, Ali Can Savas, Anjie Lu, Larissa Bubb, Xiao Lei, Rosa Moshirian, Wenjie Zhu, Cheng Peng, Taijiao Jiang, Lin Chen, Nicholas A. Graham, and Pinghui Feng

Supplemental Figures for

Title: Deamidation Shunts RelA from Mediating Inflammation to Aerobic Glycolysis

Authors: Jun Zhao,[1] Mao Tian,[1] Shu Zhang,[1] Alireza Delfarah,[2] Ruoyun Gao,[1] Youliang Rao,[1] Ali Can Savas,[1] Anjie Lu,[3] Larissa Bubb,[1] Xiao Lei,[4] Rosa Moshirian,[1] Wenjie Zhu,[5] Cheng Peng,[3] Taijiao Jiang,[5] Lin Chen,[4] Nicholas A. Graham,[2] and Pinghui Feng[1,6]*

Affiliations:

[1]Section of Infection and Immunity, Herman Ostrow School of Dentistry, Norris Comprehensive Cancer Center, University of Southern California, 925 W 34th Street, Los Angeles, CA 90089, USA;

[2]Mork Family Department of Chemical Engineering and Materials Science, Norris Comprehensive Cancer Center, 3710 McClintock Avenue, Los Angeles, CA 90089, USA;

[3]Department of Orthopedic and Plastic Surgery, The Third Xiangya Hospital of Central South University, Changsha Hunan 410013, China;

[4]Department of Molecular and Computational Biology, 1050 Childs Way, Los Angeles, CA 90089, USA;

[5]Center of Systems Medicine, Institute of Basic Medical Sciences, Chinese Academy of Medical Sciences & Peking Union Medical College, Beijing 100005, China; Suzhou Institute of Systems Medicine, Suzhou 215123, China.

[6]Lead Contact

*Correspondence: pinghuif@usc.edu

Tel: 213-764-7933

Figure S1

A

Name	Full Name	E.C.	Function
CAD	GATase, CPSase, ATCase and DHOase	6.3.5.5	Pyrimidine Biosynthesis
CTPS1 CTPS2	CTP synthase 1 CTP synthase 2	6.3.4.2	Pyrimidine Biosynthesis
PFAS	Phosphoribosylformylglycinamidine synthase	6.3.5.3	Purine Biosynthesis
GMPS	GMP synthase	6.3.5.2	Purine Biosynthesis
PPAT	Amidophosphoribosyltransferase	2.4.2.14	Purine Biosynthesis
GFPT1 GFPT2	Glutamine--fructose-6-phosphate aminotransferase	2.6.1.16	Hexosamine Biosynthesis
ASNS	Asparagine synthetase	6.3.5.4	AA Biosynthesis
NADSYN1	Glutamine-dependent NAD(+) synthetase	6.3.5.1	NAD Biosynthesis
CPS1	Carbamoyl-phosphate synthase 1	6.3.4.16	Ammonia recycling

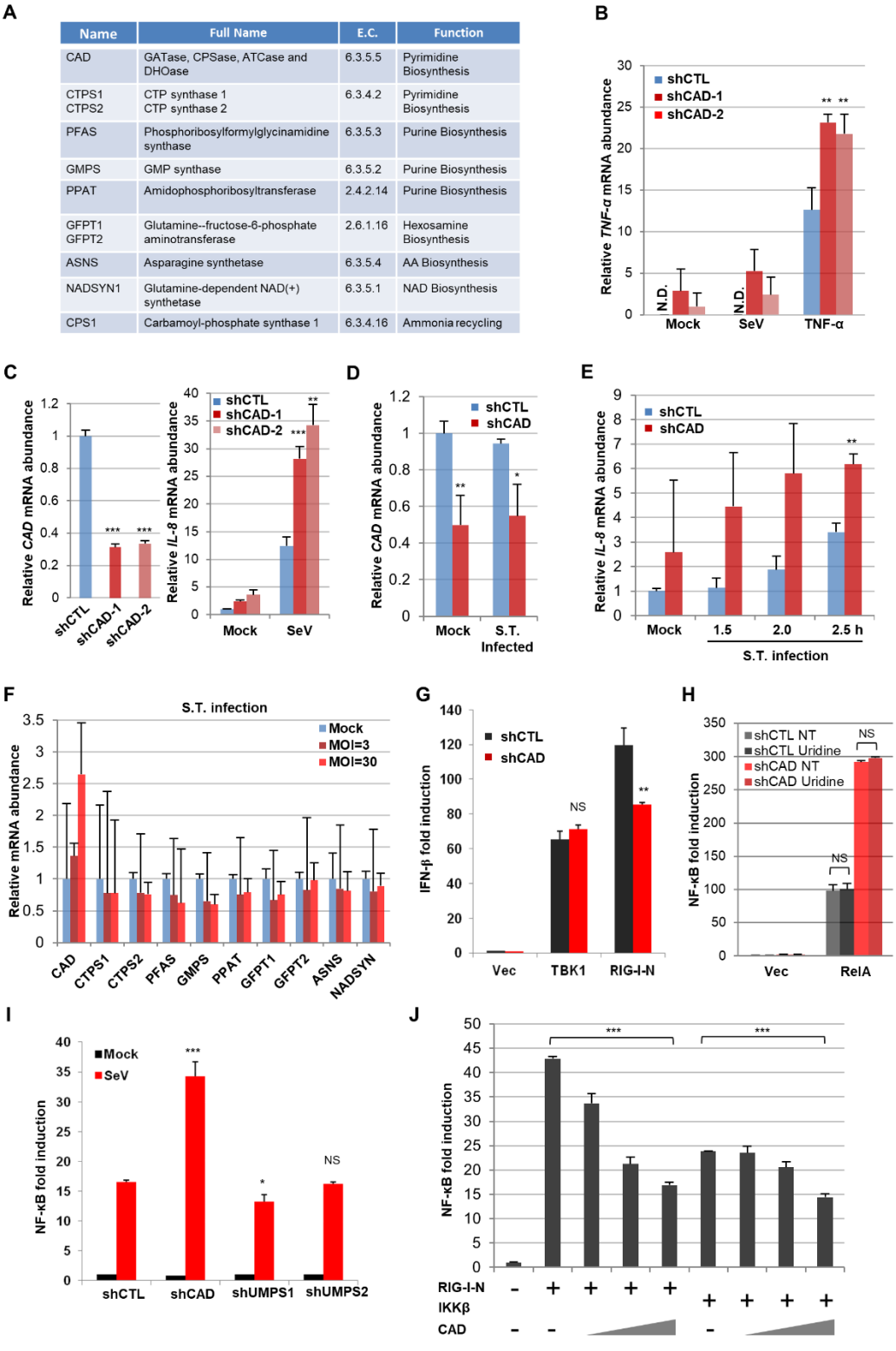

Figure S1, related to Figure 1. CAD Negatively Regulates NF-κB Activation

(A) The enzyme activity and corresponding metabolic pathway of human GATs.

(B) *TNF-α* abundance in 293T cells depleted for CAD by two different shRNAs (shCAD-1 and shCAD-2) and after infection with Sendai Virus (SeV) or treatment with TNF-α.

(C) *CAD* and *IL-8* abundance in BJ5 cells depleted for CAD by two different shRNAs (shCAD-1 and shCAD-2) and after infection with SeV.

(D and E) *CAD* (D) and *IL-8* (E) abundance in HCT116 cells depleted for CAD and after infection with *Salmonella Typhimurium* ($PhoP^c$).

(F) The mRNA abundance of indicated GATs in HCT116 cells after infection with *Salmonella Typhimurium* ($PhoP^c$).

(G) IFN-β luciferase reporter assay from 293T cells depleted for CAD and transfected with plasmids containing indicated genes.

(H) NF-κB luciferase reporter assay from 293T cells depleted for CAD, cultured with or without 10 μM of uridine, and transfected with a plasmid containing RelA.

(I) NF-κB luciferase reporter assay from 293T cells depleted for CAD or UMPS and after infection with SeV.

(J) NF-κB luciferase reporter assay from 293T cells transfected with plasmids containing IKKβ or RIG-I-N (1-200) with increasing amount of a plasmid containing CAD.

Data are presented as mean ± SD. Significance was calculated using unpaired, two-tailed Student's *t*-test. **,$P < 0.01$; ***, $P < 0.001$; NS, non-significant.

Figure S2

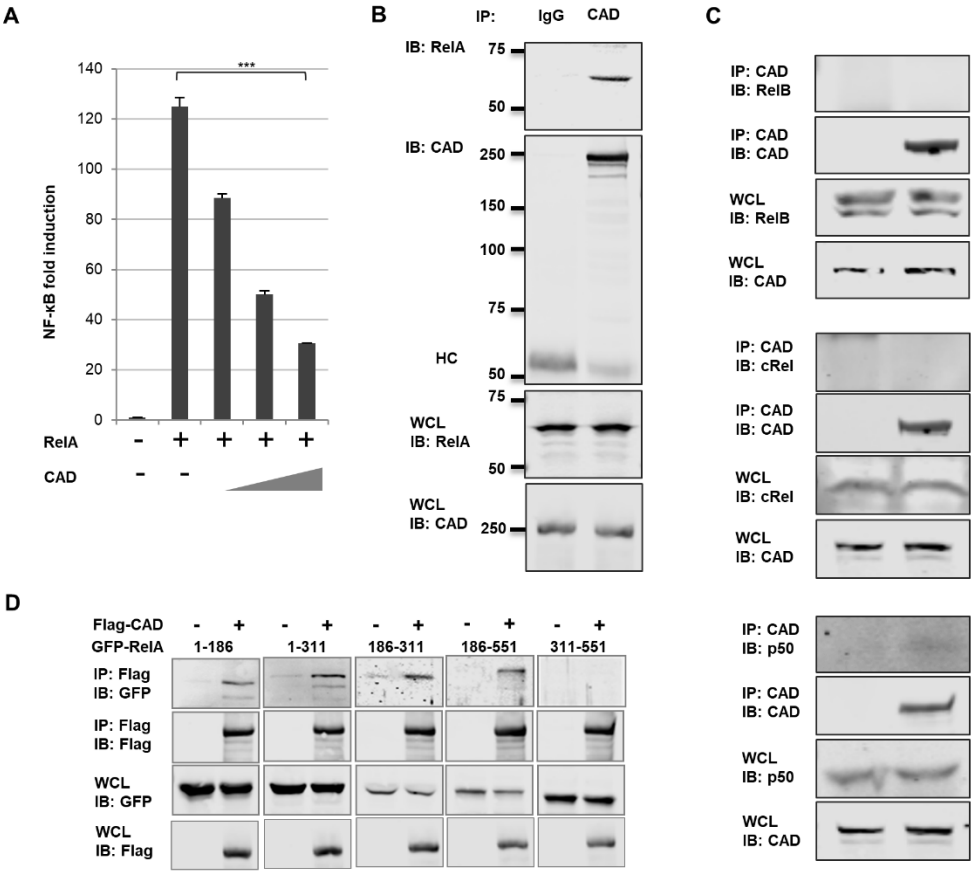

Figure S2, related to Figure 1. CAD Negatively Regulates NF-κB Activation

(A) NF-κB luciferase reporter assay from 293T cells transfected with a plasmid containing RelA and increasing amount of a plasmid containing CAD.

(B) Immunoblots of RelA and CAD from whole cell lysates (WCLs) of 293T cells precipitated with anti-CAD antibody or control (IgG) antibody. HC, heavy chain of IgG.

(C) Immunoblots of CAD, RelB (top), cRel (middle) and p50 (bottom) from WCLs of 293T cells precipitated with anti-CAD antibody or control (IgG) antibody.

(D) Immunoblots of WCLs of 293T cells transfected with plasmids containing the Flag-CAD and GFP-RelA truncation mutants and precipitated with anti-Flag antibody.

Data are presented as mean ± SD. Significance was calculated using unpaired, two-tailed Student's *t*-test. **, $P < 0.01$; ***, $P < 0.001$; NS, non-significant.

Figure S3

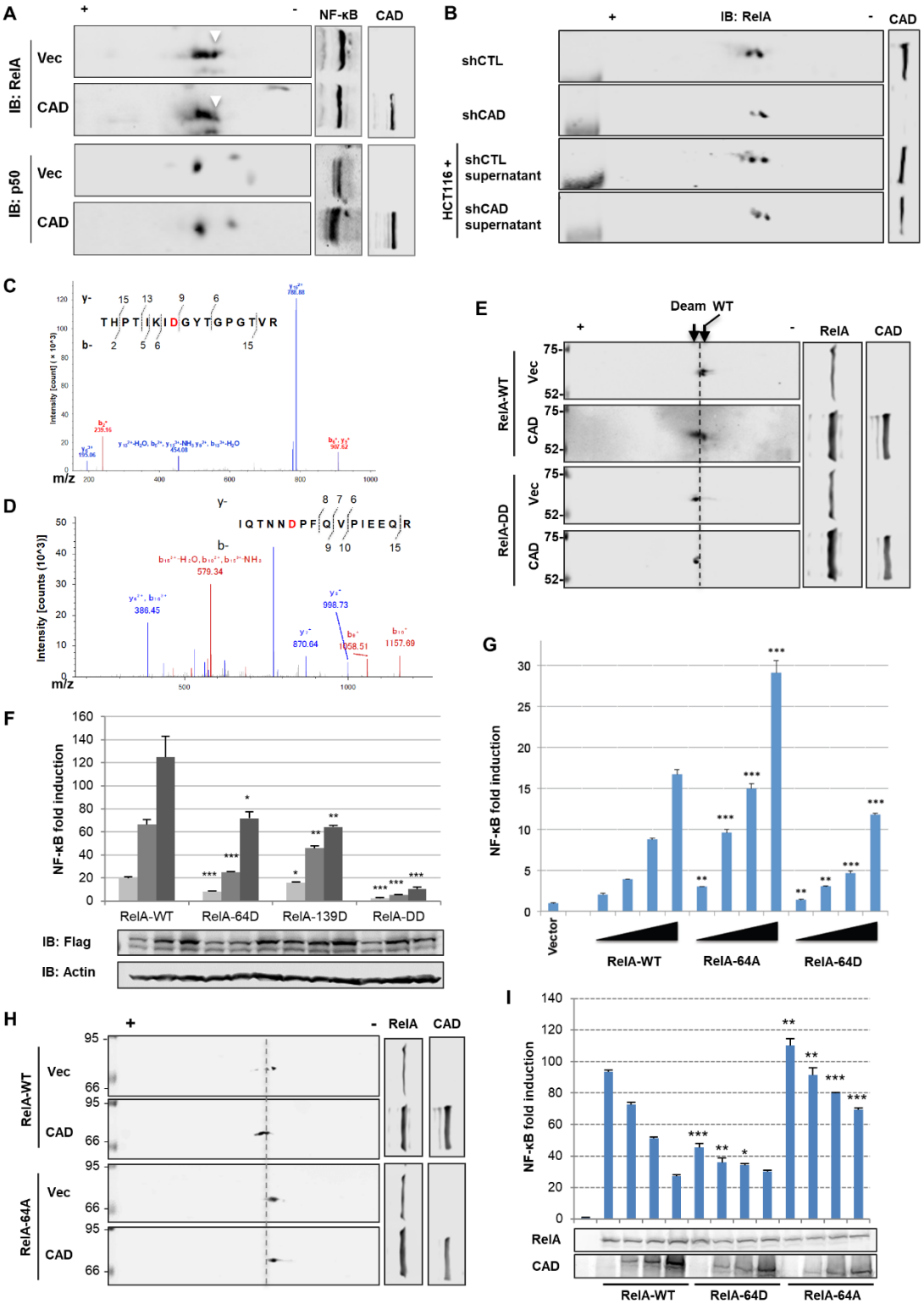
A
+
-
NF-κB
CAD
IB: RelA
Vec
CAD
IB: p50
Vec
CAD
B
+
IB: RelA
-
CAD
shCTL
shCAD
HCT116 +
shCTL supernatant
shCAD supernatant
C
y-
15 13 9 6
THPTIKIDGYTGPGTVR
b-
2 5 6 15
Intensity [count] (x 10^3)
m/z
D
y-
8 7 6
IQTNNDPFQVPIEEQR
b-
9 10 15
Intensity [counts (10^3)]
m/z
579.34
386.45
998.73
870.64
1058.51
1157.69
E
Deam WT
+
-
RelA
CAD
RelA-WT
Vec
CAD
RelA-DD
Vec
CAD
75-
52-
F
NF-κB fold induction
RelA-WT
RelA-64D
RelA-139D
RelA-DD
IB: Flag
IB: Actin
G
NF-κB fold induction
Vector
RelA-WT
RelA-64A
RelA-64D
H
+
-
RelA
CAD
RelA-WT
Vec
CAD
RelA-64A
Vec
CAD
95
66
I
NF-κB fold induction
RelA
CAD
RelA-WT
RelA-64D
RelA-64A

Figure S3, related to Figure 2. CAD Deamidates RelA to Inactivate NF-κB

(A) Immunoblots of whole cell lysates (WCLs) of HCT116 cells transfected with a plasmid containing CAD and after regular SDS-PAGE (right panels) or two-dimensional gel electrophoresis (2DGE) (left panels). Arrow denotes wild-type RelA species.

(B) Immunoblots of WCLs of HCT116 cells depleted for CAD or treated with the supernatant harvested from CAD-depleted HCT116 cells, after regular SDS-PAGE (right panels) or 2DGE (left panels) analysis.

(C and D) The m/z spectra of two peptides containing N64D (C) and N139D (D) are shown, with D highlighted in red due to deamidation, of the RelA purified from 293T cells transfected with a plasmid containing Flag-RelA with or without a plasmid containing CAD.

(E) Immunoblots of WCLs of 293T cells transfected with a plasmid containing wild-type RelA (RelA-WT) or deamidated RelA (RelA-DD) with or without CAD, after regular SDS-PAGE (right panels) or 2DGE (left panels) analysis.

(F) NF-κB luciferase reporter assay from 293T cells transfected with a plasmid containing wild-type RelA (RelA-WT), single deamidated RelA (RelA-64D and RelA-139D) or double-deamidated RelA (RelA-DD).

(G) NF-κB luciferase reporter assay from 293T cells transfected with a plasmid containing RelA-WT, deamidation-resistant RelA (RelA-64A) or RelA-64D.

(H) Immunoblots of WCLs of 293T cells transfected with a plasmid containing RelA-WT or RelA-64A with or without CAD, after regular SDS-PAGE (right panels) or 2DGE (left panels) analysis.

(I) NF-κB luciferase reporter assay from 293T cells transfected with a plasmid containing RelA-WT, RelA-N64D or RelA-64A with increasing amount of a plasmid containing CAD.

Data are presented as mean ± SD. Significance was calculated using unpaired, two-tailed Student's *t*-test. **, $P < 0.01$; ***, $P < 0.001$; NS, non-significant.

Figure S4

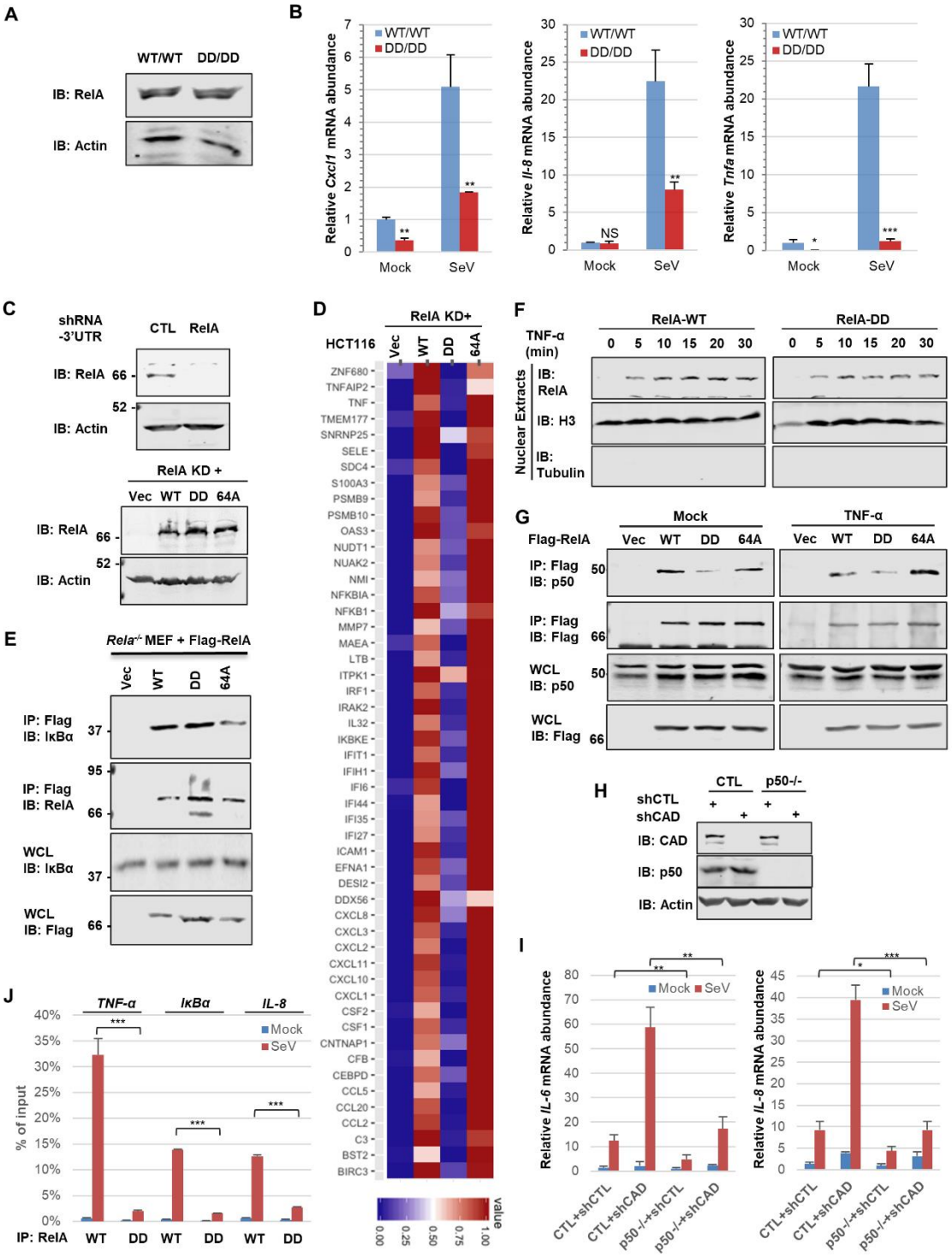
A
WT/WT
DD/DD
IB: RelA
IB: Actin
B
WT/WT
DD/DD
Relative Cxcl1 mRNA abundance
Relative IL-8 mRNA abundance
Relative Tnfa mRNA abundance
Mock
SeV
NS
C
shRNA -3'UTR
CTL
RelA
IB: RelA
IB: Actin
RelA KD +
Vec
WT
DD
64A
D
RelA KD+
HCT116
ZNF680
TNFAIP2
TNF
TMEM177
SNRNP25
SELE
SDC4
S100A3
PSMB9
PSMB10
OAS3
NUDT1
NUAK2
NMI
NFKBIA
NFKB1
MMP7
MAEA
LTB
ITPK1
IRF1
IRAK2
IL32
IKBKE
IFIT1
IFIH1
IFI6
IFI44
IFI35
IFI27
ICAM1
EFNA1
DESI2
DDX56
CXCL8
CXCL3
CXCL2
CXCL11
CXCL10
CXCL1
CSF2
CSF1
CNTNAP1
CFB
CEBPD
CCL5
CCL20
CCL2
C3
BST2
BIRC3
value
F
RelA-WT
RelA-DD
TNF-α (min)
Nuclear Extracts
IB: RelA
IB: H3
IB: Tubulin
G
Mock
TNF-α
Flag-RelA
IP: Flag IB: p50
IP: Flag IB: Flag
WCL IB: p50
WCL IB: Flag
E
Rela-/- MEF + Flag-RelA
IP: Flag IB: IκBα
IP: Flag IB: RelA
WCL IB: IκBα
WCL IB: Flag
H
CTL
p50-/-
shCTL
shCAD
IB: CAD
IB: p50
IB: Actin
I
Relative IL-6 mRNA abundance
Relative IL-8 mRNA abundance
CTL+shCTL
CTL+shCAD
p50-/-+shCTL
p50-/-+shCAD
J
TNF-α
IκBα
IL-8
% of input
IP: RelA
WT
DD

Figure S4, related to Figure 2. CAD Deamidates RelA to Inactivate NF-κB

(A) Immunoblots of whole cell lysates (WCLs) of mouse embryonic fibroblasts (MEFs) obtained at Day 14 from mouse embryos of wild-type and RelA-DD knock-in C57BL/6 mice.

(B) *Cxcl1*, *Il-8* and *Tnfa* abundance in MEFs as shown in (A) after infection with Sendai Virus (SeV).

(C) Immunoblots of WCLs of HCT116 cells depleted for endogenous RelA (top) and reconstituted with exogenous RelA-WT, RelA-DD or RelA-64A (bottom).

(D) A heatmap representing NF-κB-dependent gene expression from the RNA-sequencing analysis of reconstituted HCT116 cells as shown in (C).

(E) Immunoblots of WCLs of RelA-WT, RelA-DD or RelA-64A reconstituted *Rela*$^{-/-}$ MEFs precipitated with anti-Flag antibody.

(F) Immunoblots of the nuclear extract from *Rela*$^{-/-}$ MEFs reconstituted with RelA-WT and RelA-DD after treatment with mouse TNF-α.

(G) Immunoblots of WCLs of reconstituted HCT116 cells as described in (C) after treatment with TNF-α and precipitation with anti-Flag antibody.

(H) Immunoblots of WCLs of control (CTL) or p50-knockout 293T cells depleted for CAD.

(I) *IL-6* and *IL-8* abundance in control (CTL) or p50-knockout 293T cells depleted for CAD as shown in (H) after infection with SeV.

(J) Quantification of the promoter DNA from WCLs of reconstituted MEFs as shown in (E) after infection with SeV and precipitation with anti-Flag antibody.

Data are presented as mean ± SD. Significance was calculated using unpaired, two-tailed Student's *t*-test. **, $P < 0.01$; ***, $P < 0.001$; NS, non-significant.

Figure S5

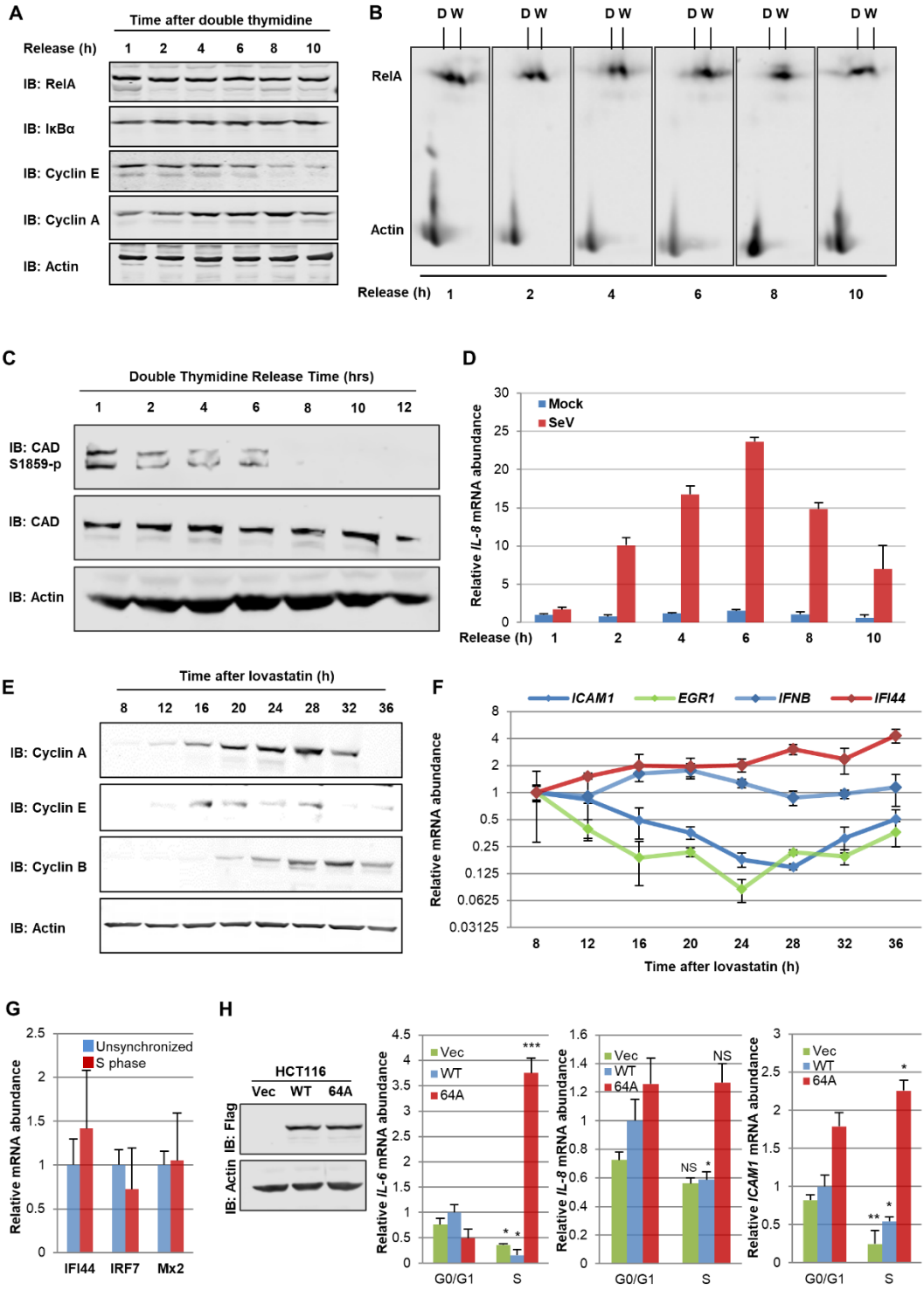
A
Time after double thymidine
Release (h) 1 2 4 6 8 10
IB: RelA
IB: IκBα
IB: Cyclin E
IB: Cyclin A
IB: Actin
B
D W D W D W D W D W D W
RelA
Actin
Release (h) 1 2 4 6 8 10
C
Double Thymidine Release Time (hrs)
1 2 4 6 8 10 12
IB: CAD S1859-p
IB: CAD
IB: Actin
D
Mock
SeV
Relative IL-8 mRNA abundance
Release (h) 1 2 4 6 8 10
E
Time after lovastatin (h)
8 12 16 20 24 28 32 36
IB: Cyclin A
IB: Cyclin E
IB: Cyclin B
IB: Actin
F
ICAM1 EGR1 IFNB IFI44
Relative mRNA abundance
Time after lovastatin (h)
G
Unsynchronized
S phase
Relative mRNA abundance
IFI44 IRF7 Mx2
H
HCT116
Vec WT 64A
IB: Flag
IB: Actin
Vec
WT
64A
Relative IL-6 mRNA abundance
Relative IL-8 mRNA abundance
Relative ICAM1 mRNA abundance
G0/G1 S
NS
***
**
*

Figure S5, related to Figure 3. RelA Deamidation and NF-κB Downregulation is Cell Cycle-dependent

(A and B) Immunoblots of whole cell lysates (WCLs) from HCT116 cells released at indicated time points after double thymidine block analyzed by regular SDS-PAGE (A) or two-dimensional gel electrophoresis (2DGE) (B). D: deamidated; W: wild-type.

(C) Immunoblots of WCLs from HCT116 cells released at indicated time points after double thymidine block.

(D) *IL-8* abundance in HCT116 cells after infection with SeV at indicated time points upon double thymidine block release.

(E) Immunoblots of WCLs from BJ5 cells released at indicated time points after lovastatin arrest.

(F) The mRNA abundance of *ICAM1, EGR1, IFN-β* and *IFI44* in human BJ5 foreskin fibroblasts at indicated time points as shown in (E).

(G) The mRNA abundance of *IFI44, IRF7* and *Mx2* in HCT116 cells without or with synchronization to S phase by double thymidine block.

(H) Immunoblots of WCLs from HCT116 cells stably expressing control, RelA-WT or RelA-64A (left panel). The mRNA abundance of *IL-6*, *IL-8* and *ICAM1* in HCT116 stable cells synchronized to G0/G1 and S phase by lovastatin arrest and double thymidine block, respectively (right panels).

Data are presented as mean ± SD. Significance was calculated using unpaired, two-tailed Student's *t*-test. **, $P < 0.01$; ***, $P < 0.001$; NS, non-significant.

Figure S6

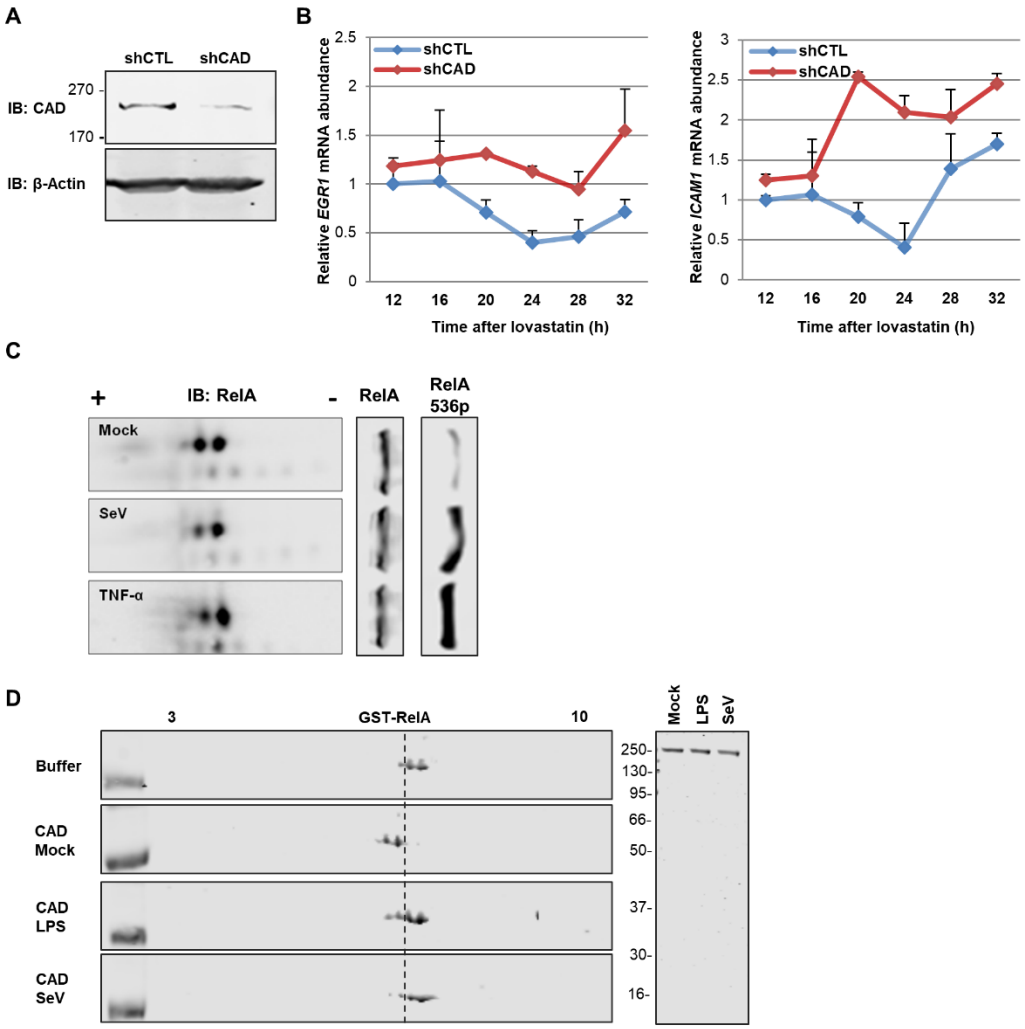

Figure S6, related to Figure 3. RelA Deamidation and NF-κB Downregulation is Cell Cycle-dependent

(A and B) Immunoblots of the whole cell lysates (WCLs) from HCT116 cells depleted for CAD (A). The mRNA abundance of *EGR1* and *ICAM1* in HCT116 stable cells released at indicated time points after lovastatin arrest (B).

(C) Immunoblots of the WCLs from HCT116 cells after infection with Sendai Virus (SeV) or treatment with TNF-α by regular SDS-PAGE and two-dimensional gel electrophoresis (2DGE) analysis.

(D) Immunoblots of in vitro deamidation reactions with GST-RelA and precipitated CAD from HCT116 Flag-CAD knockin cells that were mock-, LPS-treated or infected with SeV by 2DGE analysis (left panel). Silver stains of purified CAD (right panel).

Data are presented as mean ± SD.

Figure S7

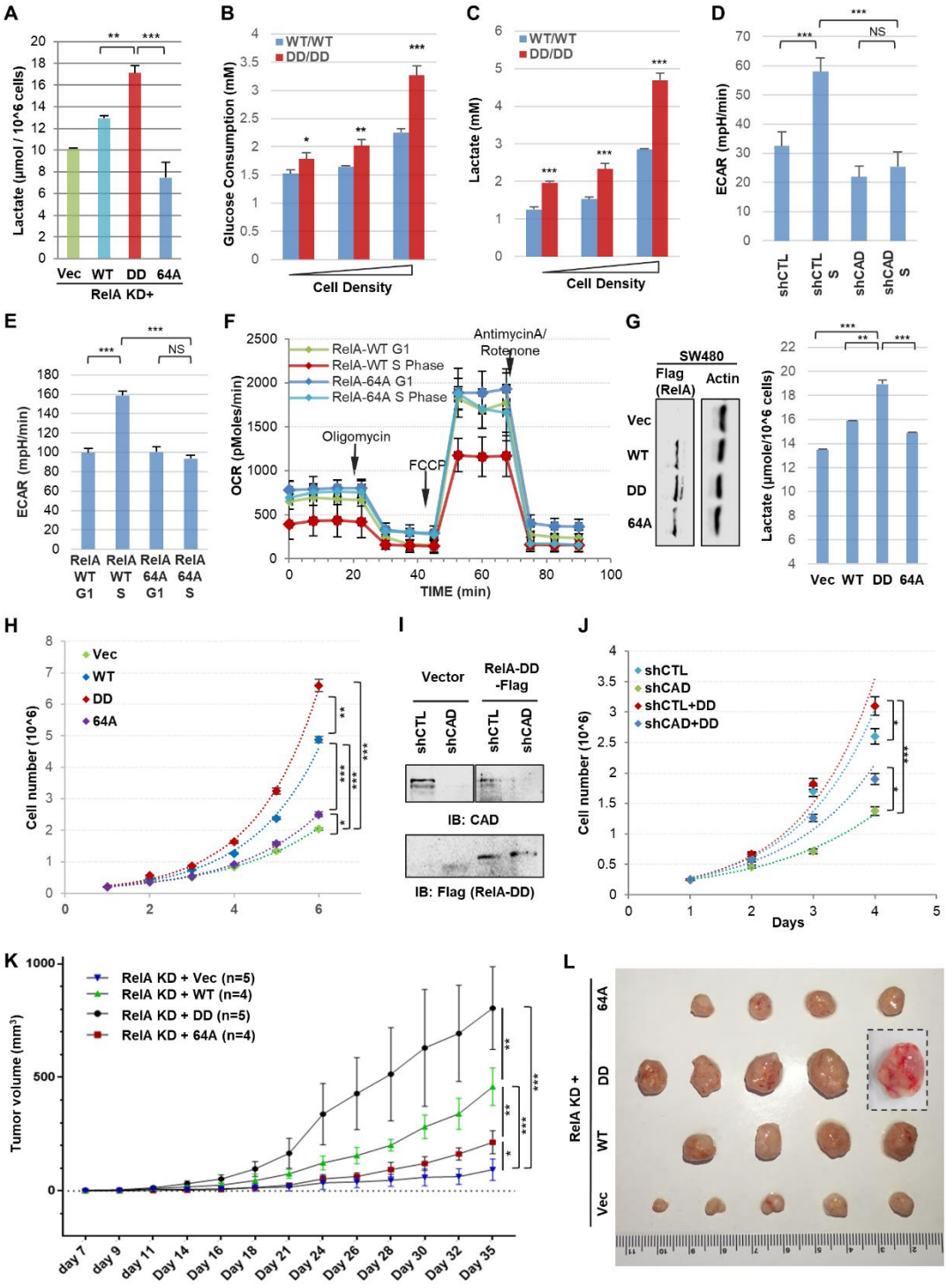
A
Lactate (µmol / 10^6 cells)
Vec WT DD 64A
RelA KD+
B
WT/WT
DD/DD
Glucose Consumption (mM)
Cell Density
C
WT/WT
DD/DD
Lactate (mM)
Cell Density
D
ECAR (mpH/min)
shCTL
shCTL S
shCAD
shCAD S
NS
E
ECAR (mpH/min)
RelA WT G1
RelA WT S
RelA 64A G1
RelA 64A S
NS
F
RelA-WT G1
RelA-WT S Phase
RelA-64A G1
RelA-64A S Phase
Oligomycin
FCCP
AntimycinA/ Rotenone
OCR (pMoles/min)
TIME (min)
G
SW480
Flag (RelA)
Actin
Vec
WT
DD
64A
Lactate (µmole/10^6 cells)
Vec WT DD 64A
H
Vec
WT
DD
64A
Cell number (10^6)
I
Vector
RelA-DD -Flag
shCTL
shCAD
shCTL
shCAD
IB: CAD
IB: Flag (RelA-DD)
J
shCTL
shCAD
shCTL+DD
shCAD+DD
Cell number (10^6)
Days
K
RelA KD + Vec (n=5)
RelA KD + WT (n=4)
RelA KD + DD (n=5)
RelA KD + 64A (n=4)
Tumor volume (mm³)
day 7
day 9
day 11
Day 14
Day 16
Day 18
Day 21
Day 24
Day 26
Day 28
Day 30
Day 32
Day 35
L
RelA KD +
64A
DD
WT
Vec

Figure S7, related to Figure 4. CAD-mediated RelA Deamidation is Crucial for Glycolysis and Cell Proliferation

(A) Lactate levels in the medium harvested from RelA-knockdown (RelA-KD) HCT116 cells reconstituted with control (vec), wild-type RelA (WT), RelA-DD (DD) and the deamidation-resistant RelA-64A (64A).

(B and C) Glucose consumption in the medium harvested from mouse embryonic fibroblasts (MEFs) of wild-type and RelA-DD knockin genotype (B). Lactate levels in the medium (C).

(D) Resting extracellular acidification rate (ECAR) of the non-synchronized or S phase synchronized HCT116 cells depleted for control or CAD.

(E) Resting ECAR of G1/S phase synchronized HCT116 cells stably expressing RelA-WT or RelA-64A.

(F) Oxygen consumption rate (OCR) of G1/S phase synchronized HCT116 cells stably expressing RelA-WT and RelA-64A.

(G) Immunoblots of WCLs from RelA-depleted SW480 cells reconstituted with RelA-WT, RelA-DD or RelA-64A (left panel), and lactate levels in the medium from reconstituted SW480 cells (right panel).

(H) Proliferation rate of reconstituted SW480 cells as shown in (G).

(I and J) Immunoblots of whole cell lysates (WCLs) from control or CAD-depleted HCT116 cells reconstituted with vector or RelA-DD (I), and proliferation rate of reconstituted HCT116 cells (J).

(K) Tumor growth in mice inoculated with reconstituted HCT116 as shown in (A).

(L) Tumors derived from reconstituted HCT116 cells. One of the tumors derived from HCT116 cells reconstituted with RelA-DD was harvested at day 30 due to ulceration.

Data are presented as mean ± SD. Significance was calculated using unpaired (paired for Figure S7H, S7J and S7K), two-tailed Student's *t*-test. **, $P < 0.01$; ***, $P < 0.001$; NS, non-significant.

Figure S8

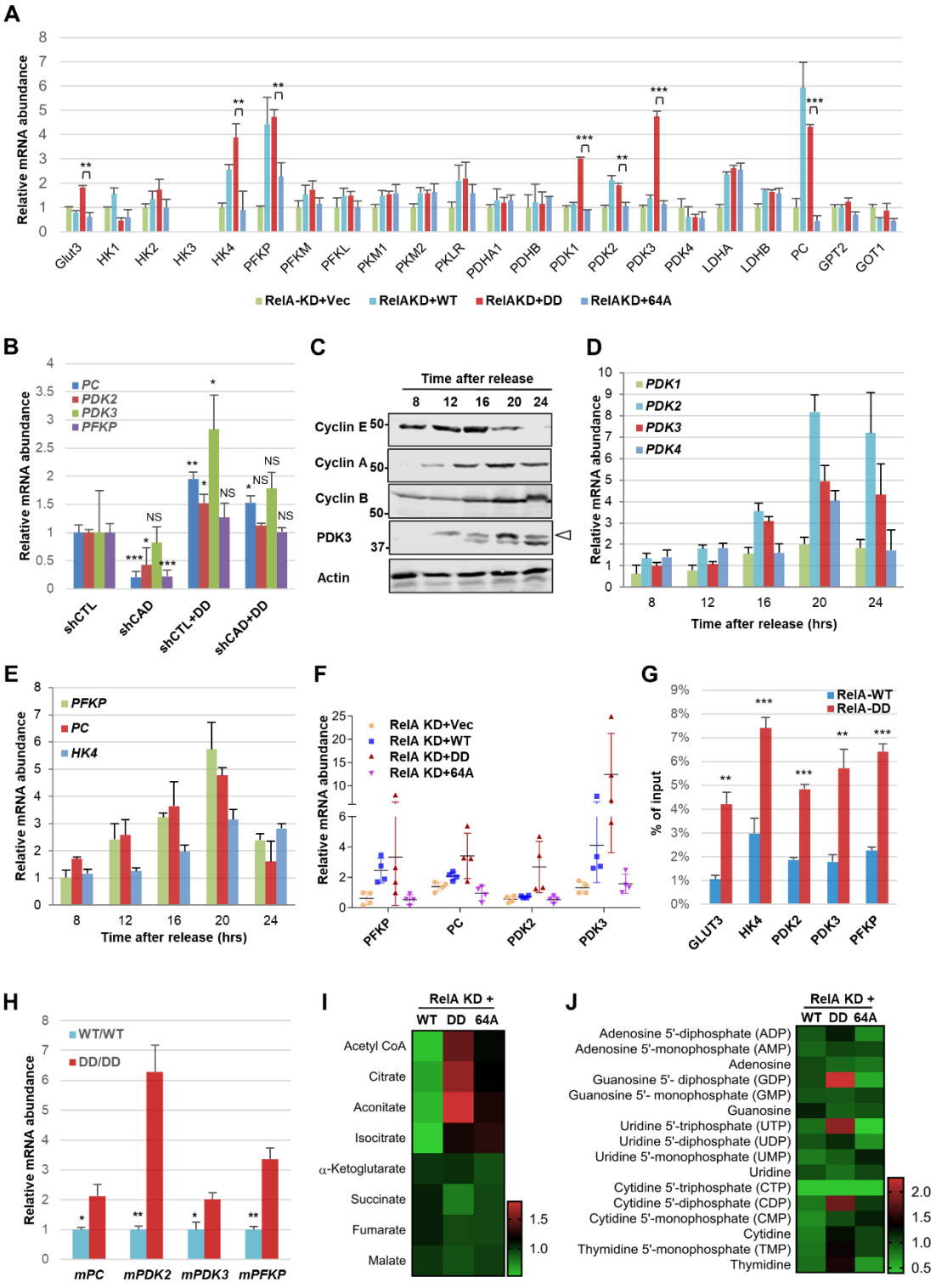
A
Relative mRNA abundance
Glut3
HK1
HK2
HK3
HK4
PFKP
PFKM
PFKL
PKM1
PKM2
PKLR
PDHA1
PDHB
PDK1
PDK2
PDK3
PDK4
LDHA
LDHB
PC
GPT2
GOT1
RelA-KD+Vec
RelAKD+WT
RelAKD+DD
RelAKD+64A
B
PC
PDK2
PDK3
PFKP
shCTL
shCAD
shCTL+DD
shCAD+DD
C
Time after release
8
12
16
20
24
Cyclin E
Cyclin A
Cyclin B
PDK3
Actin
D
PDK1
PDK2
PDK3
PDK4
Time after release (hrs)
E
PFKP
PC
HK4
Time after release (hrs)
F
RelA KD+Vec
RelA KD+WT
RelA KD+DD
RelA KD+64A
PFKP
PC
PDK2
PDK3
G
RelA-WT
RelA-DD
% of input
GLUT3
HK4
PDK2
PDK3
PFKP
H
WT/WT
DD/DD
mPC
mPDK2
mPDK3
mPFKP
I
RelA KD +
WT DD 64A
Acetyl CoA
Citrate
Aconitate
Isocitrate
α-Ketoglutarate
Succinate
Fumarate
Malate
J
RelA KD +
WT DD 64A
Adenosine 5'-diphosphate (ADP)
Adenosine 5'-monophosphate (AMP)
Adenosine
Guanosine 5'- diphosphate (GDP)
Guanosine 5'- monophosphate (GMP)
Guanosine
Uridine 5'-triphosphate (UTP)
Uridine 5'-diphosphate (UDP)
Uridine 5'-monophosphate (UMP)
Uridine
Cytidine 5'-triphosphate (CTP)
Cytidine 5'-diphosphate (CDP)
Cytidine 5'-monophosphate (CMP)
Cytidine
Thymidine 5'-monophosphate (TMP)
Thymidine

Figure S8, related to Figure 5. Metabolic Reprogramming by Deamidated RelA

(A) The mRNA abundance of glycolytic genes in reconstituted HCT116 cells.

(B) The mRNA abundance of *PC*, *PDK2*, *PDK3* and *PFKP* in control or CAD-depleted HCT116 cells reconstituted with vector or RelA-DD.

(C - E) Immunoblots of whole cell lysates (WCLs) of HCT116 cells at indicated time points released from lovastatin arrest (C). The mRNA abundance of *PDKs* and indicated glycolytic genes in HCT116 cells at indicated time points released from lovastatin arrest (D, E).

(F) The mRNA abundance of *PFKP*, *PC*, *PDK2* and *PDK3* in tumors derived from reconstituted HCT116 cells.

(G) Quantification of the promoter sequence of indicated genes in WCLs of reconstituted HCT116 cells precipitated with anti-Flag antibody.

(H) The mRNA abundance of *PFKP*, *PC*, *PDK2* and *PDK3* in mouse embryonic fibroblasts (MEFs) of wild-type and RelA-DD knock-in.

(I and J) A heatmap showing the intracellular concentration of metabolic intermediates of the TCA cycle (I) and nucleotide (J) analyzed by the metabolite profiling of reconstituted HCT116 cell lines.

Data are presented as mean ± SD. Significance was calculated using unpaired, two-tailed Student's *t*-test. **, $P < 0.01$; ***, $P < 0.001$; NS, non-significant.

Figure S9

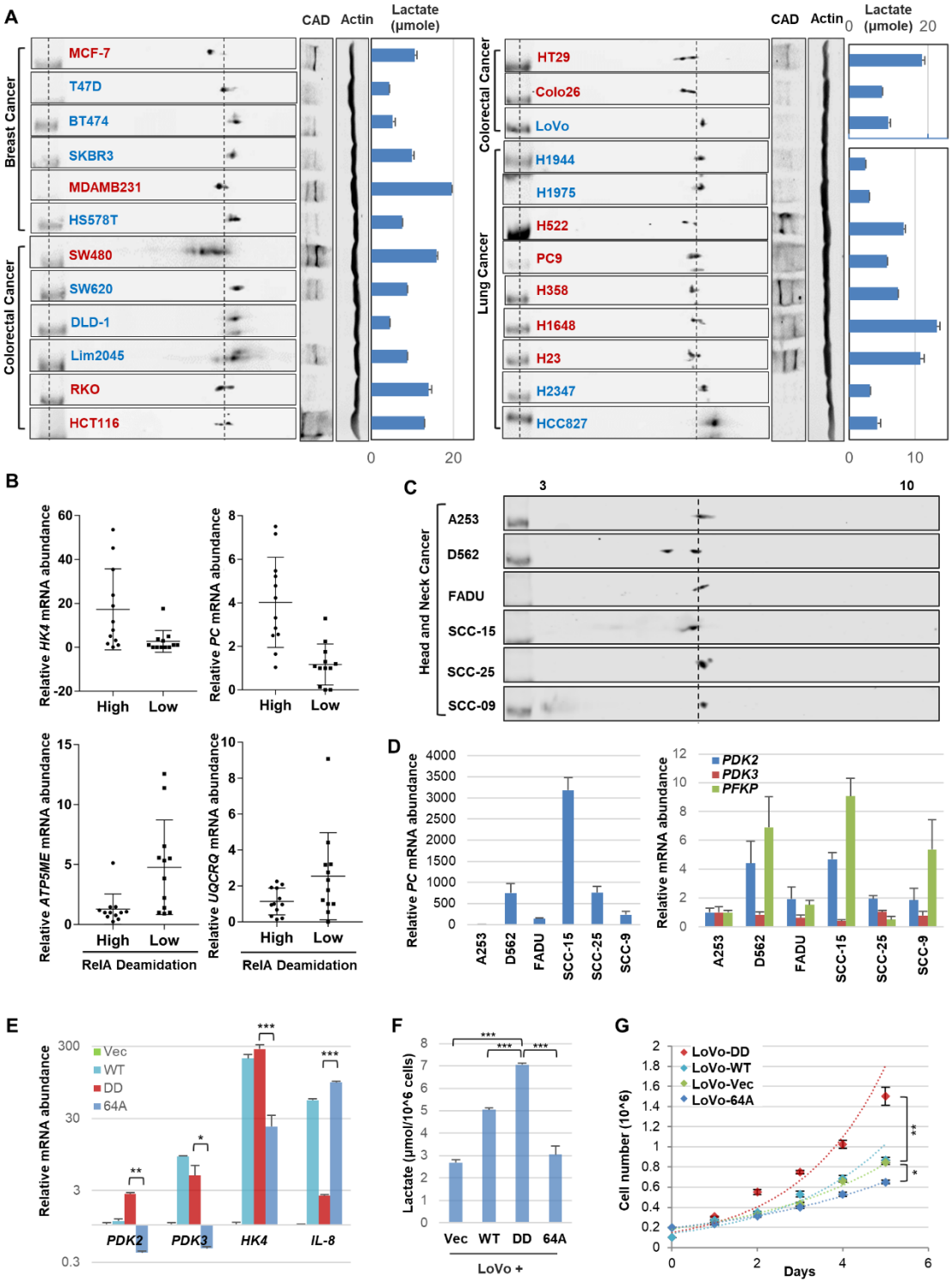
A
CAD
Actin
Lactate (μmole)
Breast Cancer
MCF-7
T47D
BT474
SKBR3
MDAMB231
HS578T
Colorectal Cancer
SW480
SW620
DLD-1
Lim2045
RKO
HCT116
Colorectal Cancer
HT29
Colo26
LoVo
Lung Cancer
H1944
H1975
H522
PC9
H358
H1648
H23
H2347
HCC827
0
20
0
10
B
Relative HK4 mRNA abundance
Relative PC mRNA abundance
Relative ATP5ME mRNA abundance
Relative UQCRQ mRNA abundance
High
Low
RelA Deamidation
C
3
10
Head and Neck Cancer
A253
D562
FADU
SCC-15
SCC-25
SCC-09
D
Relative PC mRNA abundance
Relative mRNA abundance
PDK2
PDK3
PFKP
A253
D562
FADU
SCC-15
SCC-25
SCC-9
E
Relative mRNA abundance
Vec
WT
DD
64A
PDK2
PDK3
HK4
IL-8
F
Lactate (μmol/10^6 cells)
Vec
WT
DD
64A
LoVo +
G
Cell number (10^6)
LoVo-DD
LoVo-WT
LoVo-Vec
LoVo-64A
Days

Figure S9, related to Figure 6. CAD-mediated RelA Deamidation is Crucial for Diverse Human Cancer Cells

(A) Immunoblots for RelA deamidation and CAD expression, and lactate production of twenty-four cancer cell lines of breast, colon and lung origin. These cell lines were then classified into high RelA deamidation (Red) and low or no RelA deamidation groups (Blue).

(B) The mRNA abundance of *HK4*, *PC*, *ATP5ME* and *UQCRQ* in the 24 cancer cell lines as described in (A) classified into high RelA deamidation and low or no RelA deamidation groups.

(C and D) Immunoblots of six human head and neck cancer cell lines for RelA deamidation analyzed by two-dimensional gel electrophoresis (C). The mRNA abundance of *PC*, *PDK2*, *PDK3* and *PFKP* in head and neck cancer cells (D).

(E - G) The mRNA abundance of *PDK2*, *PDK3*, *HK4* and *IL-8* in LoVo colorectal cancer cells reconstituted with wild-type RelA, RelA-DD and RelA-64A (E), and lactate levels in the medium (F) and proliferation rate (G) of reconstituted LoVo cells.

Data are presented as mean ± SD. Significance was calculated using unpaired, two-tailed Student's *t*-test. **, $P < 0.01$; ***, $P < 0.001$; NS, non-significant.

Figure S10

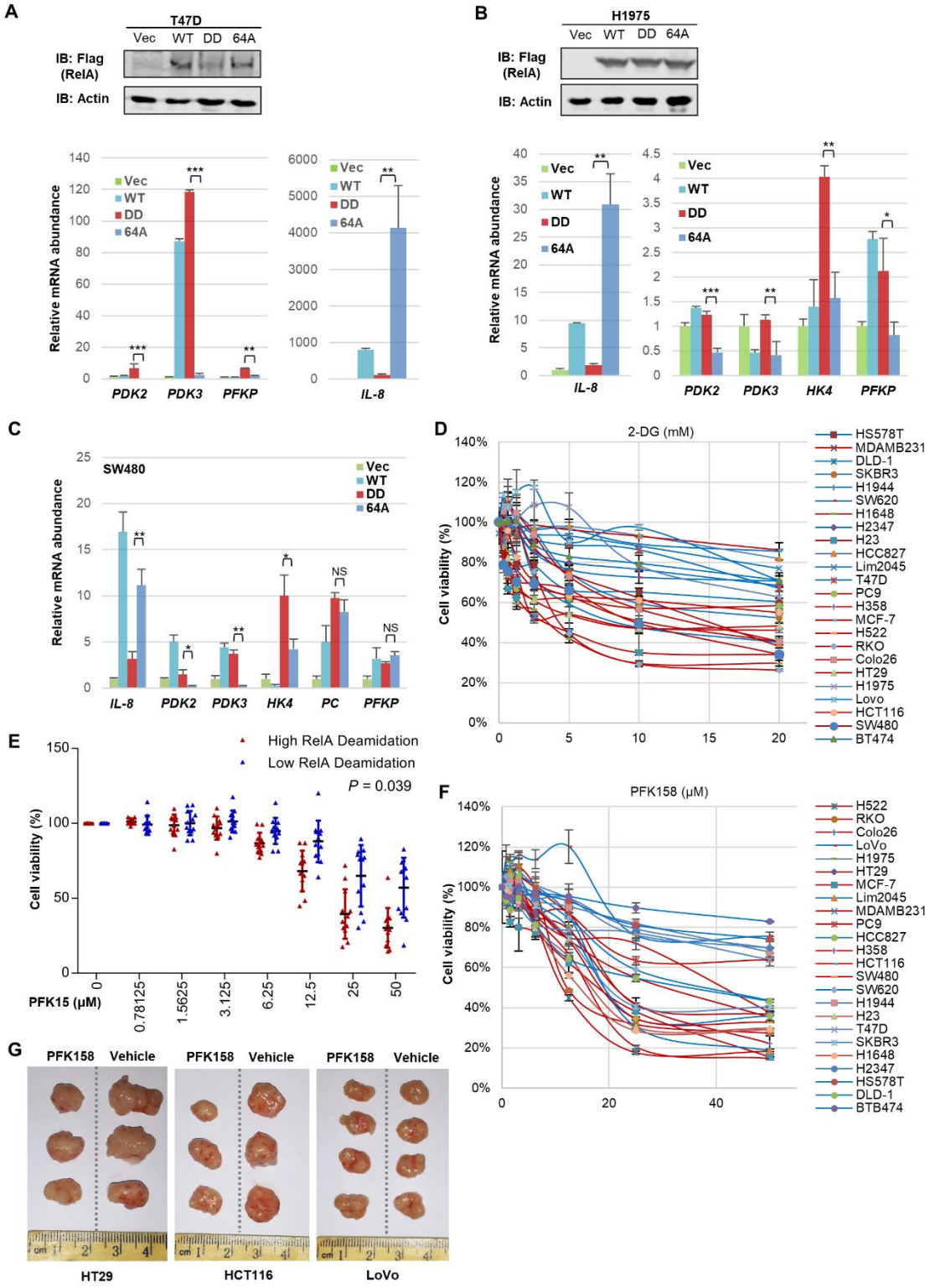
A
T47D
Vec WT DD 64A
IB: Flag (RelA)
IB: Actin
Relative mRNA abundance
Vec
WT
DD
64A
PDK2
PDK3
PFKP
IL-8
B
H1975
Vec WT DD 64A
IB: Flag (RelA)
IB: Actin
Relative mRNA abundance
IL-8
PDK2
PDK3
HK4
PFKP
C
SW480
Relative mRNA abundance
IL-8
PDK2
PDK3
HK4
PC
PFKP
NS
D
2-DG (mM)
Cell viability (%)
HS578T
MDAMB231
DLD-1
SKBR3
H1944
SW620
H1648
H2347
H23
HCC827
Lim2045
T47D
PC9
H358
MCF-7
H522
RKO
Colo26
HT29
H1975
Lovo
HCT116
SW480
BT474
E
High RelA Deamidation
Low RelA Deamidation
P = 0.039
Cell viability (%)
PFK15 (μM)
F
PFK158 (μM)
Cell viability (%)
H522
RKO
Colo26
LoVo
H1975
HT29
MCF-7
Lim2045
MDAMB231
PC9
HCC827
H358
HCT116
SW480
SW620
H1944
H23
T47D
SKBR3
H1648
H2347
HS578T
DLD-1
BTB474
G
PFK158
Vehicle
HT29
HCT116
LoVo

Figure S10, related to Figure 6. CAD-mediated RelA Deamidation is Crucial for Diverse Human Cancer Cells

(A) Immunoblots of whole cell lysates (WCLs) from T47D breast cancer cells reconstituted with wild-type RelA, RelA-DD and RelA-64A (top panel). The mRNA abundance of *PDK2*, *PDK3*, *PFKP* and *IL-8* in reconstituted T47D cells (bottom panel).

(B) Immunoblots of whole cell lysates (WCLs) from H1975 lung cancer cells reconstituted with wild-type RelA, RelA-DD and RelA-64A (top panel). The mRNA abundance of *IL-8*, *PDK2*, *PDK3*, *PFKP* and *HK4* in reconstituted H1975 cells (bottom panel).

(C) The mRNA abundance of *IL-8*, *PDK2*, *PDK3, HK4, PC and PFKP* in the SW480 cells depleted for endogenous RelA and reconstituted with wild-type RelA, RelA-DD and RelA-64A.

(D) Cell viability of 24 human cancer cell lines treated with 2-DG. Red and blue lines denote individual data point of cancer cell lines with high and low levels of RelA deamidation, respectively.

(E and F) Cell viability of the panel of 24 cancer cell lines treated with PFK-158 (a PFKFB3 inhibitor), plotted as the mean of a group (E) and individual cell line (F). Red: High deamidation cell lines. Blue: Low or no deamidation cell lines.

(G) Representative tumors derived from HT29, HCT116 and LoVo colorectal cancer cells in nude mice, treated with vehicle or PFK158 (25 mg/kg) (n = 6 for both treated groups).

Data are presented as mean ± SD. Significance was calculated using unpaired (paired for Figure S10E), two-tailed Student's *t*-test. **, $P < 0.01$; ***, $P < 0.001$; NS, non-significant.

TABLE S1, related to METHODS DETAILS

Gene Name	Forward Primer	Reverse Primer
Realtime PCR primers		
Human CAD	5'-TGCTCACCTATCCTCTGATCG-3'	5'-GCTGGGAGTAGGACAGCAC-3'
Human CCL2	5'-AAGATCTCAGTGCAGAGGCTCG-3'	5'-TTGCTTGTCCAGGTGGTCCAT-3'
Human EGR1	5′-CTCTCCAGCCTGCTCGTC-3′	5′-AGCAGCATCATCTCCTCCAG-3′
Human GOT1	5'-ACCTGGGAGAATCACAATGC-3'	5'-GCGGCTGTGCCCGCCGGTGC-3'
Human GOT2	5'-CAATGGCTGCAAGAAGTGAA-3'	5'-GGCTTTAGCCCTGTGAAACA-3'
Human GPT2	5'-GGAGCTAGTGACGGCATTTCTACGA-3'	5'-CCCAGGGTTGATTATGCAGAGCA-3'
Human HK1	5'-GGTGAAATCGTCCGCAAC-3'	5'-CCCGGGTCTT CATCGTC-3'
Human HK2	5'-CGGCCGTGCTACAATAGG-3'	5'-CTCGGGATCATGTG AGGG-3'
Human ICAM-1	5'-GGCCGGCCAGCTTATACAC-3'	5'-TAGACACTTGAGCTCGGGCA-3'
Human IFI44	5′-CCACCGAGATGTCAGAAAGAG -3′	5′-TGGTACATGTGGCTTTGCTC -3′
Human IFNB	5'-AGGACAGGATGAACTTTGAC-3'	5'-TGATAGACATTAGCCAGGAG-3'
Human IL-6	5'-CCAGCTATGAACTCCTTCTC - 3'	5'-GCTTGTTCCTCACATCTCTC - 3'
Human IL-8	5'-GGCACAAACTTTCAGAGACAG-3'	5'-ACACAGAGCTGCAGAAATCAGG-3'
Human IRF7	5′-TGCAAGGTGTACTGGGAG-3′	5′-TCAAGCTTCTGCTCCAGCTCCATAAG-3′
Human LDHA	5′-AGCCCGATTCCGTTACCT-3′	5′-CACCAGCAACATTCATTCCA-3′
Human LDHB	5'-TTGTGGTTTCCAACCCAGTGGACA-3'	5'-AAAATCCATCCATGGCAGCTGCTG-3'
Human MX2	5′-AGAAATTACATTCTTTCAAACACATCC-3'	5′-GATCTCAAATGTCTTGTAGTTGACAAA-3'
Human PDK1	5'-CCGCTCTCCATGAAGCAGTT-3'	5'-TTGCCGCAGAAACATAAATGAG-3'
Human PDK2	5'-CCGCTGTCCATGAAGCAGTT-3'	5'-TGCCTGAGGAAGGTGAAGGA-3'
Human PDK3	5'-CAAGCAGATCGAGCGCTACTC-3'	5'-CGAAGTCCAGGAATTGTTTGATG-3'
Human PDK4	5'-CCCGAGAGGTGGAGCATTT-3'	5'-GCATTTTCTGAACCAAAGTCCAGTA-3'
Human PFKP	5′-CGGAAGTTCCTGGAGCACCTCTC-3′	5′-AAGTACACCTTGGCCCCCACGTA-3′
Human PKM1	5′-CTATCCTCTGGAGGCTGTGC-3′	5′-CCATGAGGTCTGTGGAGTGA-3′
Human PKM2	5′-CCACTTGCAATTATTTGAGGA A-3′	5′-GTGAGCAGACCTGCCAGACT-3′
Human PC	5′-ACCAACTGCCGTGATGCTGA-3′	5′-ACACACGGATGGCAATCTCACC-3′
Human TNF-α	5′-AGG CGC TCC CCA AGA AGA CA-3′	5′-TCC TTG GCA AAA CTG CAC CT-3′
Human β-actin	5'-CTGGCACCCAGCACAATG-3'	5'-GCCGATCCACACGGAGTACT-3'
Mouse Ccl-5	5'-CCTGCTGCTTTGCCTACCTCTC-3'	5'-ACACACTTGGCGGTTCCTTCGA-3'
Mouse Mip2	5'-CTCTCAAGGGCGGTCAAAAAGTT-3'	5'-TCAGACAGCGAGGCACATCAGGTA-3'
Mouse β-actin	5'-ACGGCCAGGTCATCACTATTG-3'	5'-CAAGAAGGAAGGCTGGAAAAGA-3'
Human DDX60	5'-AAGGTGTTCCTTGATGATCTCC-3'	5'-TGACAATGGGAGTTGATATTCC-3'
Human Glut3	5'-CAGCGAGACCCAGAGATG-3'	5'-TTGGAAAGAGCCGATTGTAG-3'
Human HK3	5'-CTCCAGGCTGGTGTCAGTGA-3′	5'-CTCCGATTGCAAAAAGGTGACT-3′
Human HK4	5'-GCTTGTGATTCTGGGATGGA-3'	5'-GCTATGGGAGCTGAAGATGTAG-3'
Human PFKM	5'-GAGTGACTTGTTGAGTGACCTCCAGAAA-3′	5'-CACAATGTTCAGGTAGCTGGACTTCG-3′
Human PFKL	5'-GGCATTTATGTGGGTGCC AAAGTC-3′	5'-CAGTTGGCCTGCTTGATGTTCTCA-3′
Human PKLR	5'-GAAAGGCCCAAGGTATCCAA-3'	5'-GCAGAGTGAGGGTGGTAAAG-3'
Human PDHA1	5'-GTTACCACGGACACAGTATGAG-3'	5'-CATCCTGTCCTTGAGAAGCATAA-3'
Human PDHB	5'-GGAGTAGGAGCTGAAATCTGTG-3'	5'-GCATAAGGCATAGGGACATCA-3'
Human PC	5′-GATAGTGTCTGCCTTCTGGAGAGC-3′	5′-ACACACGGATGGCAATCTCACC-3′
Human GPT	GGAGCTAGTGACGGCATTTCTACGA-3′	5'-CCCAGGGTTGATTATGCAGAGCA-3'
Human ATP5ME	5'-GAGAAGGCACCGTCGATGG-3′	5'-ACACTCTGAATAGCTGTAGGGAT-3′
Human UQCRQ	5'-TGGTGGAGTCTTGCACTAAAG-3'	5'-CTCCTGGCACAGAAACAGAA-3'
ChIP-PCR primers		
Human TNF-α	5'-GATTCCTTGATGCCTGGGTGTC-3′	5'-GAGCTTCTGCTGGCTGGCTGT-3′
Human IκBα	5'-GCTTCTCAGTGGAGGACGAG-3′	5'-CTGGCAGGGGATTTCTCAG-3′

TABLE S1, related to METHODS DETAILS

Human IL-8	5'-GTGTGATGACTCAGGTTTGCCC-3′	5'-GTGTGATGACTCAGGTTTGCCC-3′
Human GLUT3	5'-CCCCTGAAGCAATCTTGTGATC-3'	5'-AAAAACCCAGGGTGGAGAGAG-3'
Human HK4	5'-AACTTTGGTGTGACCCTTAC-3'	5'-CCAAAGCATCTACCTCTTAGC-3'
Human PDK2	5'-CCGGAGTTGTTTGTGAGTGG-3'	5'-GCCTCCTCCCTACCCTTG-3'
Human PDK3	5'-CCGGACAAAACACAAACGTC-3'	5'-CAGCAGCAGCTCCAGGAC-3'
Human PFKP	5'-TCATCTCTAGAGCCCCCAAC-3'	5'-GTGTGGGCAGGAGCATCTAC-3'
sgRNA		
Human CAD	5’-ACCTGTCTTTGGGATCTGCCTGG-3’	Exon 6
Human CAD	5’-GAACGGCATGTACATCCGCATGG-3’	Exon 43
Human NF-κB1	5’-TGTGAAGGCCCATCCCATGGTGG-3’	Exon 5